R. M. Andrews and M. W. Brown†*

Elevated Temperature Out-of-Phase Fatigue Behaviour of a Stainless Steel

REFERENCE Andrews, R. M. and Brown, M. W., **Elevated temperature out-of-phase fatigue behaviour of a stainless steel**, *Biaxial and Multiaxial Fatigue*, EGF 3 (Edited by M. W. Brown and K. J. Miller), 1989, Mechanical Engineering Publications, London, pp. 641–658.

ABSTRACT Out-of-phase multiaxial low cycle fatigue tests have been conducted on a type 316 stainless steel at 550°C, under fully reversed strain-controlled tension–torsion loading for a range of biaxialities and phase angles. Fatigue endurance is shown to be reduced for the case of non-proportional loading below the level predicted by the ASME Boiler and Pressure Vessel Design Code.

Correlation of the empirical fatigue lives is examined in terms of both the plastic work theory and the critical shear plane approach to low cycle fatigue, but with limited success. Therefore, two alternative phenomenological parameters are proposed, which are specifically designed to incorporate non-proportional loading effects. These are assessed not only for the austenitic steel tested here, but also against published data for a ferritic steel.

Introduction

Multiaxial low cycle fatigue has received a great deal of attention in a variety of research schools over the past twenty years. It has become apparent that one of the more intractable problems associated with complex load systems is that of non-proportional straining. This is not merely an academic problem but one of practical concern that must be addressed in any design code of general applicability (**1**). Non-proportional strain paths occur, firstly, in situations where the three principal strains do not remain in constant ratios of proportionality throughout a complete strain cycle, and, secondly, when the principal axes of stress and strain do not remain in fixed space but rotate markedly during a cycle. Load histories that must be classified as non-proportional are observed in a variety of engineering components, and one notable case is that of combined bending and torsion in beams and shafts.

A study of the literature shows that few multiaxial studies concern non-proportional problems, e.g., see references (**2**)–(**16**). A useful review article by Garud (**11**) demonstrates the need for a satisfactory method of general applicability with which to assess the severity of loading under complex stressing. The present paper reviews non-proportional data in the low-cycle fatigue regime with specific reference to high temperature behaviour. A series of experiments from tension–torsion tests on AISI 316 stainless steel at 550°C

* Now at The Welding Institute, Abington Hall, Abington, Cambridge CB1 6AL, UK.
† Mechanical Engineering Department, University of Sheffield, Mappin Street, Sheffield S1 3JD, UK.

are presented and the results are used to assess three correlation procedures previously used. Finally a new method is developed that specifically incorporates the deformation behaviour observed in non-proportional loading.

Notation

b	Material constant
F	Rotation factor, see equation (5)
j	Material constant
N_f	Fatigue endurance
S	Material constant
W_p^*	Plastic strain energy function
γ	Torsional shear strain
$\bar{\gamma}$	Effective shear strain
γ_{max}	Maximum shear strain
γ_p	Torsional plastic strain
Δ	Range of strain
ε	Axial strain
$\varepsilon_1, \varepsilon_2, \varepsilon_3$	Principal strains
ε_n	Normal strain on maximum shear plane
ε_p	Axial plastic strain
ε_T	'Total' strain, see equation (1)
λ	Biaxiality factor, $\Delta\gamma/\Delta\varepsilon$
ν	Effective Poisson's ratio
σ	Axial stress
τ	Torsional stress
ϕ	Phase angle

Low cycle fatigue under non-proportional loading

Most reported non-proportional data are derived from room temperature tests, in the high cycle fatigue area. Quantitative comparisons are made difficult due to the use of different specimen geometries, failure definitions, and test methods. Inconsistent presentation of the data also obscures trends; for example, plotting torsion and tensile results directly, rather than converting to (say) maximum shear strain.

The earliest low cycle tension–torsion work at room temperature was that of Zamrik and Frishmuth (**2**) on 7075-T6 aluminium alloy. They tested tubular specimens in displacement controlled fully reversed tension, torsion and biaxial combinations. The original data (**3**) showed biaxialities ranging from $\lambda = 0.81$ to $\lambda = 6.90$. The biaxiality λ is defined as the ratio of torsional shear strain range to axial strain range, $\Delta\gamma/\Delta\varepsilon$. Tests were not concentrated at specific biaxialities, and so these results are difficult to re-analyse. Phase angles of 0, 30, 45, 60, and 90 degrees were used. A 'total strain', defined as the greatest value in the cycle of

$$\varepsilon_T = \sqrt{(\varepsilon_1^2 + \varepsilon_2^2 + \varepsilon_3^2)} \quad (1)$$

was used to correlate the results. Here ε_1, ε_2, and ε_3 are the principal strains. Scatter at low lives (<100 cycles) was attributed to buckling. A 90 degree phase shift gave points on the lower edge of the scatter band.

Kanazawa *et al.* (**4**) tested a 1 per cent Cr–Mo–V bainitic steel in tension–torsion at room temperature at biaxialities of 1.0, 1.5, 2.0, and 4.0. Various phase angles were tested at $\lambda = 1.5$ and 4.0, but only 90 degrees was employed at $\lambda = 1.0$ and 2.0. Both maximum shear strain range, $\Delta\gamma_{max}$, and maximum octahedral shear strain range failed to correlate the results. At $\lambda = 1.5$ and 4.0, life decreased as the phase angle increased from 0 to 90 degrees. By interpolating between data points to obtain the life corresponding to a maximum shear strain range of 3 per cent, they plotted life against the amplitude of the normal strain on the maximum shear plane, ε_n. A correlation within a factor of 40 per cent on life was obtained. It was stated that the relative phase of γ_{max} and ε_n did not significantly affect life.

Jordan *et al.* (**5**) used the same specimen geometry and material when extending this work. They used a continuous torsion cycle with short (one tenth period) axial half cycles applied at specific points in the torsion cycle. The applied strain amplitudes, the maximum shear strain and the maximum normal strain were kept the same for all tests. The fatigue life was approximately constant for different positions of the axial spike in the torsion cycle. This supported the suggestion that the relative phase of γ_{max} and ε_n does not affect life. When compared with the data of Kanazawa *et al.* (**4**), these tests fell above the line for 'ordinary' out-of-phase tests to show enhanced endurance. Reducing the normal strain amplitudes by a factor of 0.5 brought the points onto the line.

It was concluded that amplitudes alone are insufficient to correlate endurance, but the paths taken by normal and shear strains throughout a cycle must also be considered. Physically, this implies that the normal strain 'damages' the material continuously throughout the cycle. Therefore, this effect was included by using a root mean square value of ε_n obtained by integrating over one half cycle. The effective strain of Kandil *et al.* (**6**)–(**8**) was then used to correlate the data with that of Kanazawa (**4**) and the room temperature data of Brown (**9**)(**10**). A correlation within a factor of 50 per cent on life was obtained. However, the characteristic exponent for the material used in the effective strain definition ($j = 0.55$) was substantially different from that of the in phase data alone ($j = 2.5$). Jordan's results were also analysed by Garud's plastic work method (**11**)(**12**), giving a similar correlation on life.

Sonsino and Grubisic's (**13**) tests on solid specimens of 321 stainless steel and an alloy steel gave endurances (to the formation of a 1 mm crack) in the range 1000–200 000 cycles. For both materials a 90 degree phase shift gave the lowest endurance. Graphs were derived to show the influence of phase angle on the applied strain amplitudes required for a life of 10 000 cycles. The alloy steel

30CrNiMo8 (with UTS 1030 MPa) required an 8 per cent reduction in strain at 90 degree phase shift; for AISI 321, the reduction was 14 per cent.

Taira *et al.* tested a 0.16 per cent carbon steel at 450°C (**14**) in tension–torsion at a phase shift of 90 degrees only. The phase shift reduced life, even when the data were presented using a von Mises correlation. A slightly improved correlation was obtained from a 'damage' model where the effective strain was integrated around the cycle.

Ohnami *et al.* (**15**)(**16**) tested tubular specimens of AISI 304 at 550 and 650°C. Alternate axial and torsional strain controlled cycles were used, together with push–pull, torsion, and in-phase biaxial cycling. A small starter hole caused rapid crack initiation. At 550°C alternate push–pull and torsion cycles gave reduced lives and a fivefold increase in measured crack growth rates compared with in-phase biaxial cycling. Crack growth was transgranular in all cases. However, fatigue life was not affected by changing from biaxial to alternate cycling at 650°C, and crack growth rates only increased slightly. This was attributed to a change of fatigue mechanism to intergranular fracture.

Material and test method

Material and specimen

The material was AISI 316 stainless steel, from a reference heat known as RNL Material 83. The chemical composition and monotonic properties at 20°C and 550°C are given in Table 1. The material had been produced as 35 mm diameter bar. It was tested as received, i.e., solution annealed at 1050°C for 30 minutes and air cooled.

The tubular specimens were machined from the bar and finished by honing the bore and polishing the outer surface. The specimen design has been discussed elsewhere (**17**). The strain distribution along the gauge length was approximately uniform. Kandil (**6**) showed that the strain distribution was better for cyclic hardening materials. This specimen design was used in references (**4**)–(**10**), and so comparisons with these results should not be influenced by either specimen geometry or size effects.

Table 1 Composition (weight %) and monotonic properties for RNL Material 83, from Kandil (6)

C	*Si*	*Mn*	*Ni*	*Cr*	*Mo*	*P*	*N*	*S*	*B*
0.060	0.49	1.75	12.30	17.68	2.34	0.035	0.040	0.021	17 ppm

	Temperature	
	20°C	550°C
0.2% proof stress (MPa)	298	136
UTS (MPa)	593	465
Elongation	61	46
Reduction in area (%)	77	65

Test machine

Tests were carried out in a servo-controlled tension–torsion test machine described by Brown and Miller (**17**) although some improvements to the rig were made for this programme. The tension and torsion loads of this machine were controlled from the output of a biaxial extensometer fitted on the specimen. The command signals for each servo system were provided by a twin channel signal generator with an adjustable phase difference between the channels.

The specimen was heated by a three zone furnace. A pair of resistance coils around the ends of the specimen were each powered by a thyristor controller, using a feed back signal from a type K (chromel–alumel) thermocouple spot welded to the end of the gauge length. A third zone was provided by cartridge heaters placed in the specimen bore and operated at constant voltage. The optimum power settings for the three zones were determined in an initial calibration.

The load and strain signals were recorded continuously, and in addition load–strain hysteresis loops were plotted on x–y plotters at intervals throughout the test. The latter were used to determine load and strain ranges at half-life, corresponding to stable cyclic behaviour.

Results

All tests were performed at 550°C, using fully reversed triangular strain-controlled cycles. The biaxialities tested were 0, 1, 1.5, 2, 4, and ∞, covering the range from pure tension ($\lambda = 0$) to pure torsion ($\lambda = \infty$), using both proportional (in phase) and non-proportional (out-of-phase) tests. The phase shift ϕ in the non-proportional tests was defined such that the axial strain cycle led the torsional one.

Tests were commenced with the axial straining alone, the torsional shear strain starting from zero after the phase lag ϕ. The frequency for each test was chosen to give a maximum shear strain rate of 0.1 per cent/second. Failure was defined as the point where the load range had fallen by 2 per cent from a straight line fitted to the steady part of the load range versus number of cycles curve. The smaller number of cycles obtained from the axial and torsional curves respectively was used to determine the endurance of biaxial tests.

Endurances in the regions of 1500 cycles and 10 000 cycles, respectively, were obtained. Non-proportional loading reduced the fatigue life compared with the same strain ranges applied in phase. For constant biaxiality, the greatest reduction in endurance was at a phase shift of 90 degrees.

The in-phase tests at $\lambda = 0$, 2, and ∞ agreed well with the continuous cycling results of Kandil *et al.* (**8**) on the same material. Therefore the two sets of data were combined to increase the number of results available for analysis. The uniaxial ($\lambda = 0$) data also agreed well with other data for 316 stainless steel tested at 550°C (**18**).

The results are presented in the following sections in terms of four theories for non-proportional low cycle fatigue.

ASME Code Case N47 Equivalent Strain

The ASME Boiler and Pressure Vessel Design Code Case N47 defines an equivalent strain range together with a procedure for its evaluation under non-proportional loading situations. It is based essentially on the octahedral shear strain, but normalised to give the principal strain range under uniaxial stress low cycle fatigue conditions. To derive the radial and circumferential strains in the tubular specimen from the measured axial and torsional strains, an effective Poisson's ratio was derived from the measured stress ranges (**18**). The effective Poisson's ratio was then assumed to be constant throughout the strain cycle. The equivalent strain range can be evaluated from these four strains (see Appendix 1).

Figure 1 shows the results, where it can be seen that proportional cycling at each biaxiality gives a separate and distinct trend. The endurance increased as the biaxiality increased from push–pull to torsion. At 1500 cycles the non-proportional results all fell below the corresponding proportional results, and generally lay below the uniaxial data. The results were less clear cut at 10000 cycles, but the out-of-phase points are on the lower edge of the scatter band. There was no obvious trend at $\lambda = 1.5$, where the phase shift was varied.

Also shown on Fig. 1 is the code 'continuous cycling' design line. All the present results lie on the safe side of the line. However, this line was derived

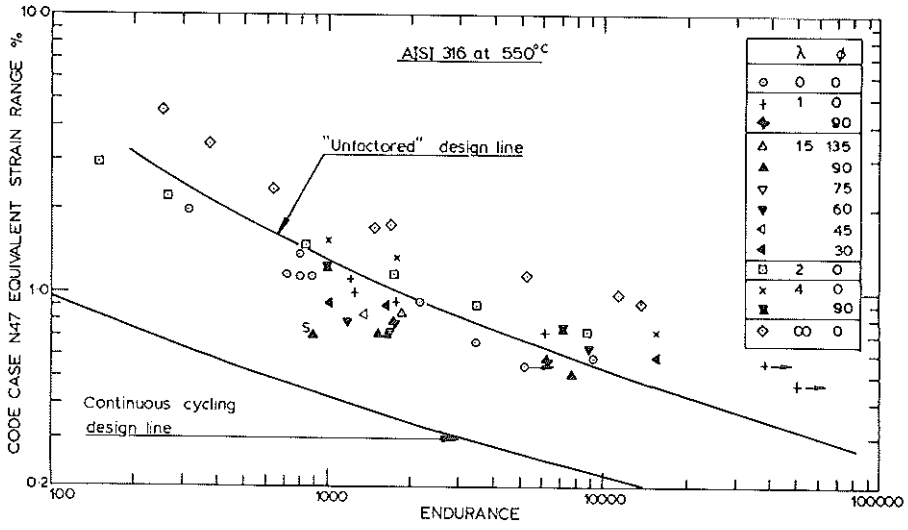

Fig 1 Results correlated using the method of ASME Code Case N47. Point 's' was a sinusoidal waveform test

from uniaxial data by applying factors of either two on strain or twenty on life, whichever gave the lower life. The continuous cyling line has been 'unfactored' to give the second line in the original data position, as shown in Fig. 1. This unfactored line passes through the proportional data, slightly above the push–pull points. A substantial part of the factoring at 1500 cycles has been used up by the change to non-proportional loading. The two run-outs at $\lambda = 1$, and some of the non-proportional tests, lie well above the unfactored line. This supports the suggestion of Wood *et al.* (**19**) that the code design line may be unnecessarily conservative at low strain levels.

Maximum plastic work correlation

This method, proposed by Garud (**11**)(**12**) uses a plastic work function given by

$$W_p^* = \oint \sigma \, d\varepsilon_p + 0.5 \oint \tau \, d\gamma_p \tag{2}$$

The work per cycle due to axial and torsional loading respectively was measured from the areas of the hysteresis loops, and converted to average energy/unit volume. The factor of 0.5 weighting the torsion work is an empirical factor introduced by Garud (**12**).

Figure 2 shows that, despite the empirical scaling factor, the pure torsion results are separated from the other data for in-phase tests. A reduction of the factor applied to the torsional work should reduce this separation. For this material a value of about 0.3 would be needed to replace 0.5 in equation (2).

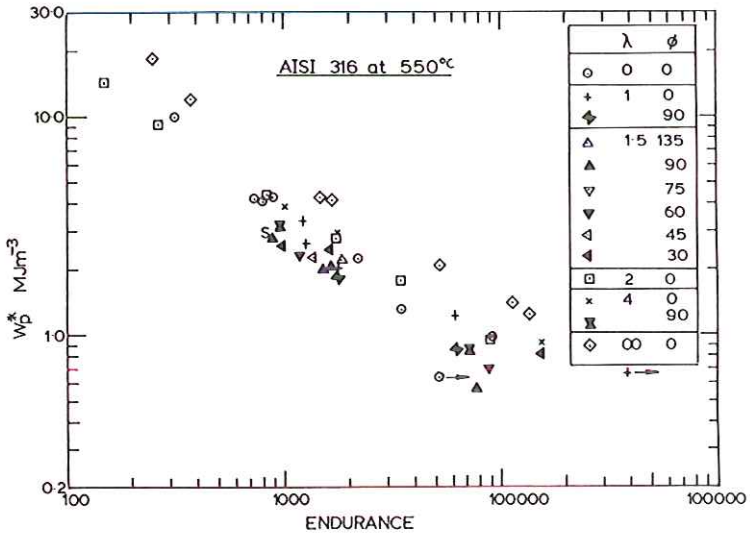

Fig 2 Results correlated using the maximum plastic work method. Point 's' was a sinusoidal waveform test

This change would also affect the biaxial results, but to a lesser extent, as the axial component of W_p^* remains unchanged. The non-proportional tests are well correlated at 1500 cycles, although they are on the low side of the scatter band. A reduction in the torsion work scaling factor would tend to move these points further below the in-phase data. At 10 000 cycles the correlation is less good. Jordan *et al.* (5) showed a similar divergence at longer lives for Kanazawa *et al.* tests (4) on 1 per cent CrMoV steel.

Correlations using the Γ plane

An effective shear strain, $\bar{\gamma}$, defined by

$$\frac{\bar{\gamma}}{2} = \frac{\gamma_{max}}{2} + S\varepsilon_n \tag{3}$$

was found to fit the in-phase test results. Here γ_{max} is the maximum shear strain amplitude and ε_n is the normal strain amplitude on the maximum shear plane. The constant S is found from the reciprocal of the slope of a constant life contour on the Γ plane of Brown and Miller (**20**). The Γ plane is a graph of ε_n vs $0.5\gamma_{max}$, on which the fatigue strength of a material under biaxial stress may be plotted. Figure 3 shows the correlation obtained, with $S = 2.42$ in equation (3), for proportional loading. The results are well correlated, and there is no separation with biaxiality. A least squares fit gave a curve for endurance N_f, where

$$\log \bar{\gamma} = 2.23 - 0.949 \log N_f + 0.0946(\log N_f)^2 \tag{4}$$

This fitted the data to within a factor of 50 per cent on life. The equation provides a rational method of finding the effective strain at a given life. The values of the constants and the quadratic form of equation (4) do not have any

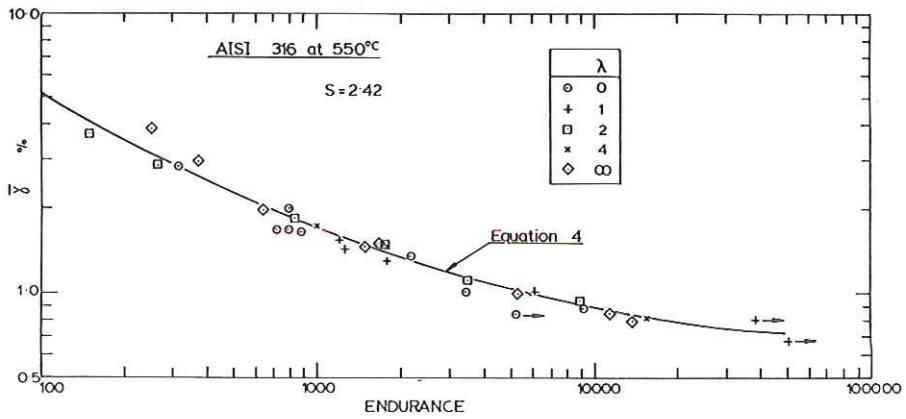

Fig 3 In-phase test results correlated by the effective total shear strain amplitude (equation (3))

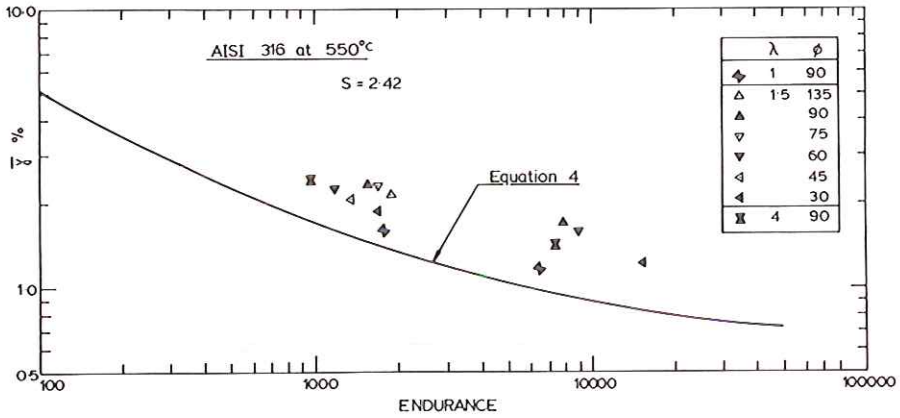

Fig 4 Out-of-phase results correlated by the effective total shear strain amplitude (equation (3)). Equation (4) represents the in-phase results

physical significance. An upper limit of $N_f = 50\,000$ cycles is an appropriate limit to the validity of this equation. The term 'effective' strain has been used to distinguish equation (3) from the 'equivalent' uniaxial strain. However, with the choice of an effective Poisson ratio, an equivalent uniaxial strain can be derived from equation (3) if desired.

Equation (3) was then applied to the out-of-phase results. The maximum shear strain range plane was identified for each test. The greatest normal strain on this plane, occurring at any time in the cycle, was then found. This peak value of ε_n does not necessarily occur at the same instant as the peak value of γ_{max}. However, Jordan *et al.* (5) showed that this phase difference did not significantly affect the endurance.

The results are shown in Fig. 4, where the out-of-phase results fall above the in-phase data represented by equation (4). Thus the correlation is very conservative, in contrast with Code Case N47 (Fig. 1) and the maximum plastic work method (Fig. 2).

Development of an effective strain for out-of-phase loading

The out-of-phase results are shown plotted on the Γ plane in Fig. 5. As with Figs 3 and 4 the ε_n values are the peak values in the cycle. The strain amplitudes plotted correspond approximately to the endurances of 1500 and 10 000 cycles, as the tests are centred around these two values (see Fig. 4). A pair of lines representing the effective strain at 1500 cycles and 10 000 cycles are shown, being derived from equations (3) and (4) to represent proportional loading behaviour.

The out-of-phase points, especially at $\lambda = 1.5$, fall outside the allowable region of the Γ plane for in-phase tests, i.e., beyond the uniaxial ($\lambda = 0$) line.

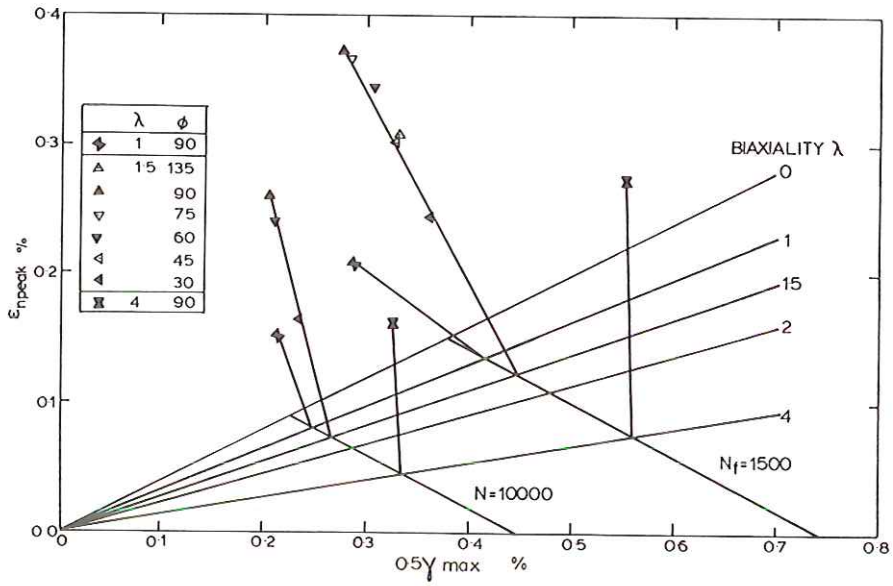

Fig 5 Γ plane showing out-of-phase results

The constant life contour for in-phase tests now has 'branches' for out-of-phase results. Figure 5 also shows that results at the same biaxiality and phase still lie on radial lines through the origin. The out-of-phase lines have been rotated away from the basic in-phase lines. At $\lambda = 1.5$ this rotation increases as the phase shift increases up to 90 degrees, but then decreases again. The amount of rotation might be used as a basis for a correlation method, but this depends on the scales at which the figure is drawn. It is not clear what the physical significance of such a method would be.

A more promising approach is to modify the normal strain ε_n to bring the points down to the in-phase effective strain contours. This is in line with Brown and Miller's original presentation (**20**) of the Γ plane. They stated that 'a secondary but important effect will be that of the tensile strain across the maximum shear-strain plane'. The out-of-phase results demonstrate this, as the increased normal strain reduces the shear strain γ_{max} for a given life.

Jordan *et al.* (**5**) used this method, albeit implicitly, when they used a root mean square value of ε_n. Because of the different axial and torsion frequencies in their tests, this was equivalent to applying a constant scale factor to the ε_n values. But they had to modify the constants of their basic correlation to incorporate the non-proportional results. A general correlation covering both in- and out-of-phase tests would be preferable.

Figure 5 shows that the amount of modification of ε_n must vary with both biaxiality and phase angle. A parameter which varies in this way is the rotation

factor F. This was introduced by Kanazawa *et al.* (**21**) when considering deformation behaviour to quantify the degree of non-proportionality in the cycle. The rotation factor F is defined by

$$F = \frac{\left\{\begin{array}{l}\text{shear strain range on plane at 45 degrees to} \\ \text{the maximum shear strain plane}\end{array}\right\}}{\{\text{maximum shear strain range}\}} \tag{5}$$

Thus a modification of equation (3) was examined, namely

$$\frac{\bar{\gamma}}{2} = \frac{\gamma_{max}}{2} + \frac{2.42\varepsilon_n}{1 + bF} \tag{6}$$

As $F = 0$ for an in-phase test, equation (6) reduces to equation (3) for proportional loading. There is an obvious similarity between this modification and the stress–strain correlation developed for out-of-phase tests by Kanazawa *et al.* (**21**).

Individual values of b were calculated for each out of phase result. To do this, equation (4) was used to find the value of $\bar{\gamma}$ corresponding to the experimental endurance. A value of F was calculated from the applied strain ranges and phase shift. These and values of γ_{max} and ε_n were substituted into equation (6) and this was solved for b. The values obtained ranged from 0.294 to 4.737, with an arithmetic mean value of 1.767. This gave a correlation

$$\frac{\bar{\gamma}}{2} = \frac{\gamma_{max}}{2} + \frac{2.42\varepsilon_n}{1 + 1.767F} \tag{7}$$

Figure 6 shows the result with the in-phase curve, equation (4), also shown. The correlation is reasonable, except at $\lambda = 1$ where the points fall well below the in-phase data.

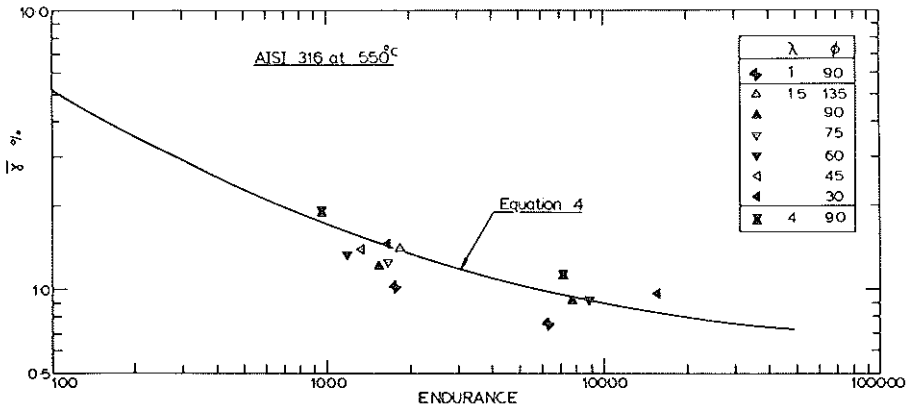

Fig 6 Effective strain correlation with a modified normal strain term, equation (7)

Table 2 Correlation constants b in equation (6) for austenitic steel

λ	b
1.0	0.38
1.5	1.61
4.0	3.87

Discussion

In developing equation (6) it was noted that individual values of b increased as the biaxiality increased. The mean values of b at each biaxiality are given in Table 2. An alternative correlation was obtained by replacing b in equation (6) with the biaxiality λ, giving for these tests

$$\frac{\bar{\gamma}}{2} = \frac{\gamma_{max}}{2} + \frac{2.42\varepsilon_n}{1 + \lambda F} \tag{8}$$

The resulting fit is shown in Fig. 7, where the correlation has improved to within a factor of two on life. The worst correlation is still at $\lambda = 1$. The use of λ avoids one disadvantage of having to determine experimentally the constant b. Taking a mean value of the individual values weights the mean value of b towards the biaxiality with the greatest number of tests, in this case $\lambda = 1.5$. Whilst this gives a good fit for these points, outlying points may be poorly correlated. Figure 6 shows this effect at $\lambda = 1$. At $\lambda = 4$ correlation is better than might be expected. However, at this biaxiality the effective strain is dominated by the shear strain, and so the modification to the normal strain is of less importance.

A criticism of the use of λ (or $\Delta\gamma/\Delta\varepsilon$) is that it is specific to the tension–torsion test system. Tests at high biaxialities might produce anomalous results due to

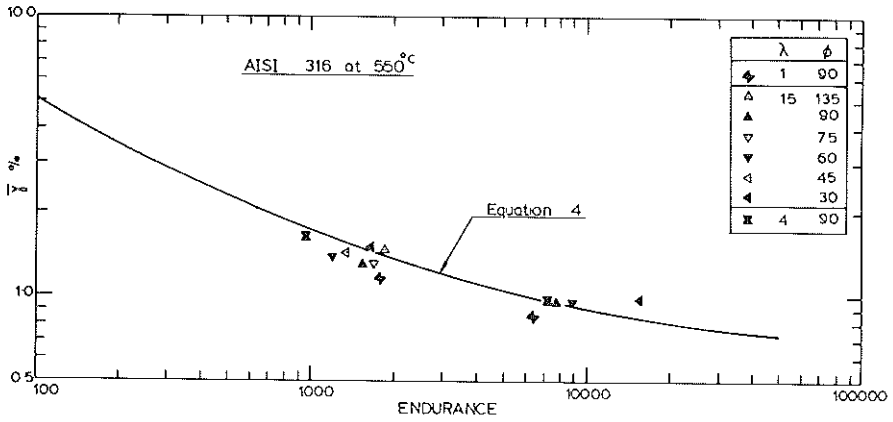

Fig 7 Improved effective strain correlation using the biaxiality factor λ, equation (8)

the large values of λ. However, a large value of λ is always associated with a small F value, and, secondly, the strain will be dominated by the shear strain component. Thus, equation (8) will probably be usable even at high biaxialities.

A more fundamental criticism of equations (7) and (8) is that the rotation factor, F, is not physically appropriate. Plasticity is a shear process on the atomic scale (**22**)–(**23**); this is incorporated into the Γ plane by using $0.5\gamma_{max}$ as the abscissa. Kanazawa *et al.* (**21**) proposed F to account for the interaction of slip systems on different shear planes under non-proportional loading. However, Brown and Miller (**20**) introduced ε_n as a secondary parameter on the Γ plane to account for effects such as fracture ductility. Thus, on physical grounds, the normal strain should be modified by a parameter reflecting fracture properties, unless the fatigue process is governed by deformation behaviour alone. (Of course deformation history may influence fracture ductility, hardened metals having reduced ductility.) The parameter must be zero for all in-phase tests, and, ideally, reach a maximum at $\lambda = 1 + \nu$, $\phi = 90$ degrees, which makes F a viable choice.

It would be possible to use a trigonometric function of ϕ, as was done by Lee (**24**). This would be completely empirical, and can only be used for simple waveforms where the phase angle is defined. Lee did not give any justification for the particular form he used.

The factor F was used here on practical grounds. It is readily calculable, and values were available from the stress–strain analysis. Successful correlation of other out-of-phase LCF data would give weight to this approach. As discussed previously, the only other available data set covering a range of biaxialities and phase angles is that of Kanazawa *et al.* (**4**)(**21**). Therefore, these data were re-analysed using this approach.

An equivalent total shear strain was derived from Brown's in-phase data for the same bainitic steel (**10**) and the in-phase data of Kanazawa *et al.* (**4**). The effective strain was defined by

$$\frac{\bar{\gamma}}{2} = \left\{\left(\frac{\gamma_{max}}{2}\right)^{2.55} + 43.2\varepsilon_n^{2.55}\right\}^{1/2.55} \tag{9}$$

The results are shown in Fig. 8; the best fit line is given by

$$\log \bar{\gamma} = 2.29 - 0.99 \log N_f + 0.0979 (\log N_f)^2 \tag{10}$$

Modifying the normal strain in the same way as in equation (6) gave

$$\frac{\bar{\gamma}}{2} = \left\{\left(\frac{\gamma_{max}}{2}\right)^{2.55} + 43.2\left(\frac{\varepsilon_n}{1 + bF}\right)^{2.55}\right\}^{1/2.55} \tag{11}$$

Individual values of b were then found using equation (10), with the same procedure as was used for the stainless steel. The mean value for the seventeen out-of-phase tests was 1.683. Figure 9 shows the results, where correlation is better than for the high temperature case in Fig. 6. This improved correlation

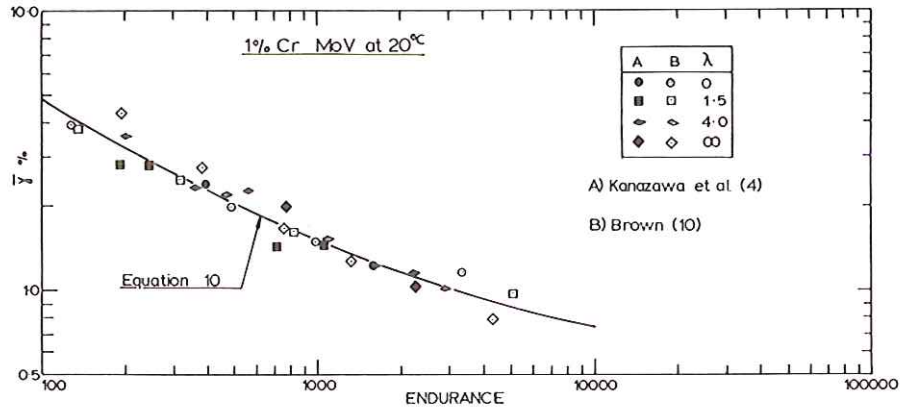

Fig 8 In-phase results for 1 per cent Cr–Mo–V steel at 20°C correlated by effective strain, equation (9)

may be due to the more even spread of biaxialities, reducing the weighting effect noted above.

Also shown is a bar representing the range of endurances of the Jordan *et al.* data (5). This has been plotted using $F = 0.65$, $\gamma_{max}/2 = 0.75$ per cent and $\varepsilon_n = 0.70$ per cent, and the lives corrected to 3 per cent maximum shear strain range. The bar is largely within a factor of two of the line fitted to the in-phase results. Note that this correlation of 'severe non-proportional loading' has been achieved using the same constants as were used for the in-phase and 'conventional' out-of-phase tests.

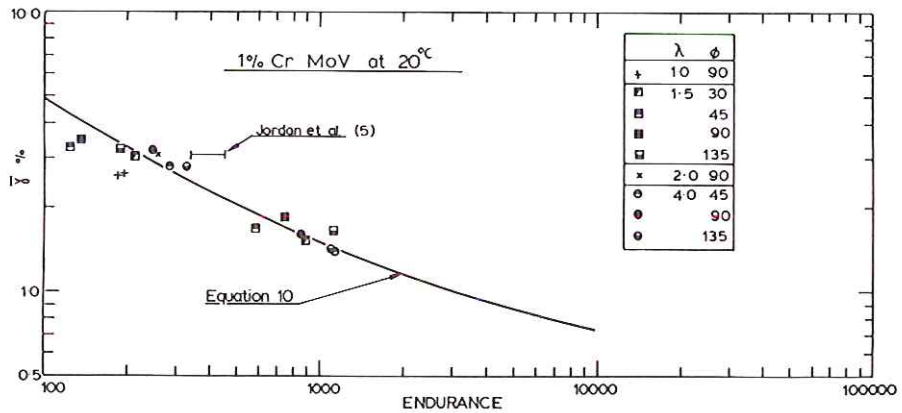

Fig 9 Out-of-phase results for 1 per cent Cr–Mo–V steel (4)(5) correlated by effective strain with a modified normal strain term, equation (11). Equation (10) represents the in-phase results

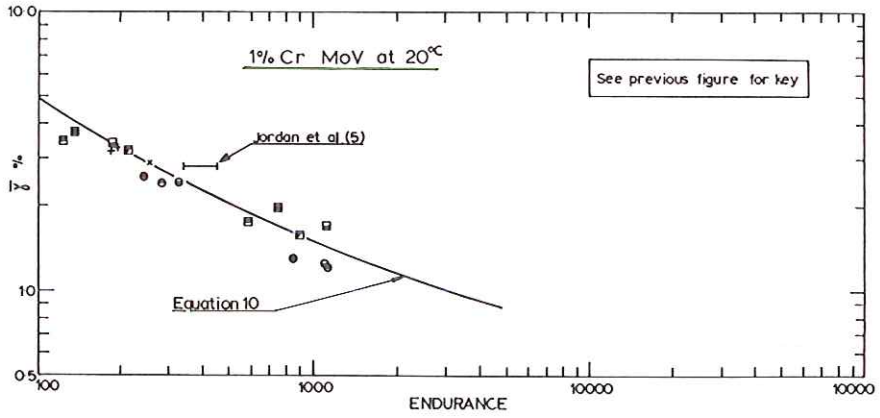

Fig 10 Improved effective strain correlation for 1 per cent Cr–Mo–V steel using the biaxiality factor λ, equation (12)

Finally, the values of b for this data also varied with the biaxiality. Mean values of b at each biaxiality are listed in Table 3. Equation (11) was modified to replace b with λ, giving

$$\frac{\bar{\gamma}}{2} = \left\{\left(\frac{\gamma_{max}}{2}\right)^{2.55} + 43.2\left(\frac{\varepsilon_n}{1 + \lambda F}\right)^{2.55}\right\}^{1/2.55} \tag{12}$$

Figure 10 shows the results; the fit has improved for low lives, especially at $\lambda = 1$, but it is worse for longer endurances.

Conclusions

(1) Non-proportional tension–torsion loading reduces fatigue life compared with proportional loading at the same maximum shear strain range.
(2) The out-of-phase test results fell below the in-phase data to give an unconservative correlation using the equivalent strain of Code Case N47.
(3) The modified maximum plastic work method correlated the out-of-phase results, but it is difficult to use in practice.
(4) When plotted on the Γ plane, non-proportional loading tests give distinct and separate contours above the in-phase tests.

Table 3 Correlation constants b in equation (11) for bainitic steel

λ	b
1.0	0.89
1.5	1.50
2.0	2.10
4.0	2.12

(5) An effective strain correlation can be devised for out-of-phase tests by modifying the normal strain with a function of phase angle.

Acknowledgements

The specimens were supplied by the United Kingdom Atomic Energy Authority. R. M. Andrews was supported by the UKAEA through a Science and Engineering Research Council Case award. M. W. Brown held a CEGB Senior Research Fellowship.

The authors are indebted to F. A. Kandil for his proportional loading data.

Appendix 1

The torsional and axial loads and strains monitored during tests may be used to derive the stress and strain conditions on the outer surface of the tubular specimens. These correspond to elastic–plastic cyclic loading so that the solution depends on the choice of a plastic flow rule, the strain hardening behaviour and a yield criterion. For proportional loading, a solution derived from the principle of maximum plastic work has been presented by Brown and Miller (**25**), which was also employed in this study. However, this method has since been extended to cover the non-proportional case by using the Prandtl–Reuss equations for plastic flow (**18**) with a Tresca yield criterion.

For the special case of the triangular waveform, the strain increments (or strain rates) and the strain amplitudes are kept in the same ratio throughout the cycle, apart from a periodic sign change. Consequently the radial distribution of stress in the tubular specimen adopts a greatly simplified form to give (**18**)

$$\sigma = Y\mu/\{\sqrt{\beta}\sqrt{(r^2 + \mu^2)}\} \tag{13}$$

$$\tau = Yr/\sqrt{(r^2 + \mu^2)} \tag{14}$$

$$Y = K\{1 + \lambda^2(r/r_o)^2/\alpha\}^{n/2} \tag{15}$$

where μ and K are constants at a given time. Here n is the cyclic strain hardening exponent and α is a function of the elasto-plastic Poisson's ratio. For a Tresca yield criterion, the constant $\beta = 0.25$. The two instantaneous constants, K and μ, are readily derived from the measured loads (**18**), after integration of the stresses over the cross-section of the specimen, using equations (13) and (14), to derive the applied load and torque.

Following the method of Brown and Miller (**25**), the factor α can be determined for proportional loading from Hencky's equations for plastic flow, to give

$$\alpha = 9\beta\{E\bar{\varepsilon}_p/\bar{\sigma} + 2(1 + \nu_e)/3\}^2/(E\bar{\varepsilon}_p/\bar{\sigma} + 1)^2 \tag{16}$$

where

$$\bar{\sigma} = \sqrt{(\sigma^2 + \tau^2/\beta)}$$

$$\bar{\varepsilon} = \sqrt{(\varepsilon^2 + \gamma^2/\alpha)}$$

and

$$\bar{\varepsilon}_p = \bar{\varepsilon} - \bar{\sigma}/E \tag{17}$$

Equation (16) is directly related to the elasto-plastic value for Poisson's ratio, which is concisely defined by the expression employed in the ASME code (**1**)

$$\nu = 0.5 - (0.5 - \nu_e)\bar{\sigma}/(E\bar{\varepsilon}) \tag{18}$$

where ν_e is the elastic value of Poisson's ratio. Solving equations (16), (17), and (18) gives

$$\alpha = 4\beta(1 + \nu)^2 \tag{19}$$

from which the value of ν may be calculated.

The value of α was found by an iterative procedure that showed very rapid convergence. Taking β as 0.25, a value confirmed by the Tresca correlation observed in proportional loading for cyclic stress–strain behaviour, the assumed initial value for α was 2.25. After solving equations (13)–(15), a new value of α was derived from equation (16) to use in the subsequent iterative step.

After convergence of α in one or two iterative steps, Poisson's ratio was determined from equation (19), and used to derive the equivalent strain

$$\varepsilon_{eq} = (\sqrt{2}/3)\{2(1 + \nu)^2\varepsilon^2 + 1.5\gamma^2\}^{1/2} \tag{20}$$

For the case of tension–torsion, this is the ASME N47 equivalent strain, as plotted in Fig. 1.

References

(1) American Society of Mechanical Engineers (1984) *Cases of the ASME Boiler and Pressure Vessel Code*; Case N47-22, ASME, New York.

(2) ZAMRIK, S. Y. and FRISHMUTH, R. E. (1973) The effects of out-of-phase biaxial strain cycling on low cycle fatigue, *Expl Mech.*, **13**, 204–208.

(3) ZAMRIK, S. Y. (1972) The effects of out-of-phase biaxial strain cycling on low cycle fatigue, NASA CR-72843.

(4) KANAZAWA, K., MILLER, K. J., and BROWN, M. W. (1977) Low cycle fatigue under out-of-phase loading conditions, *J. Eng. Mater. Technol.*, **99**, 222–228.

(5) JORDAN, E. H., BROWN, M. W., and MILLER, K. J. (1985) Fatigue under severe nonproportional loading, *Multiaxial Fatigue, ASTM STP 853*, ASTM, Philadelphia, PA, pp. 569–585.

(6) KANDIL, F. A. (1984) *Time effects on biaxial fatigue at elevated temperatures*, PhD thesis, University of Sheffield, UK.

(7) KANDIL, F. A., MILLER, K. J., and BROWN, M. W. (1982) Biaxial low cycle fatigue failure of 316 stainless steel at elevated temperature, in *Mechanical Behaviour and Nuclear Applications of Stainless Steel at Elevated Temperatures*, Metals Society, London, Book 280, pp. 203–209.

(8) KANDIL, F. A., MILLER, K. J., and BROWN, M. W. (1985) Creep and ageing interactions in biaxial fatigue of type 316 stainless steel, *Multiaxial Fatigue, ASTM STP 853*, ASTM, Philadelphia, PA, pp. 651–668.

(9) BROWN, M. W. and MILLER, K. J. (1979) High temperature low cycle biaxial fatigue of two steels, *Fatigue Engng Mater. Structures*, **1**, 217–229.
(10) BROWN, M. W. (1975) *High temperature multiaxial fatigue*, PhD thesis, Cambridge University, UK.
(11) GARUD, Y. S. (1981) Multiaxial fatigue – a survey of the state of the art, *J. Testing Eval.*, **9**, 165–178.
(12) GARUD, Y. S. (1981) A new approach to the evaluation of fatigue under multiaxial loading, *J. Engng Mater. Technol.*, **103**, 118–125.
(13) SONSINO, C. M. and GRUBISIC, V. (1985) Fatigue behaviour of cyclically softening and hardening steels under multiaxial elastic–plastic deformation, *Multiaxial Fatigue, ASTM STP 853*, ASTM, Philadelphia, PA, pp. 586–605.
(14) TAIRA, S., INOUE, T., and YOSHIDA, T. (1968) Low cycle fatigue under multiaxial stresses (in the case of combined cyclic tension–compression and cyclic torsion out-of-phase at elevated temperatures), *11th Japan Congress on Materials Behaviour*, Kyoto, pp. 60–65.
(15) OHNAMI, M., SAKANE, M., and HAMADA, N. (1985) Effect of changing principal stress axes on low cycle fatigue life in various wave shapes at elevated temperatures, *Multiaxial Fatigue, ASTM STP 853*, ASTM, Philadelphia, PA, pp. 622–654.
(16) OHNAMI, M. and HAMADA, N. (1982) Biaxial low-cycle fatigue of a SUS 304 stainless steel at elevated temperature, *25th Japan Congress on Materials Research*, Kyoto, pp. 93–99.
(17) BROWN, M. W. and MILLER, K. J. (1981) A biaxial fatigue machine for elevated temperature testing, *J. Testing Eval.*, **9**, 202–208.
(18) ANDREWS, R. M. (1986) *High temperature fatigue of AISI 316 stainless steel under complex biaxial loading*, PhD thesis, University of Sheffield, UK.
(19) WOOD, D. S., WYNN, J., BALDWIN, A. B., and O'RIORDAN, P. (1980) Some creep fatigue properties of Type 316 stainless steel at 625°C, *Fatigue Engng Mater. Structures*, **3**, 39–57.
(20) BROWN, M. W. and MILLER, K. J. (1973) A theory for fatigue failure under multiaxial stress–strain conditions, *Proc. Instn mech. Engrs*, **187**, 745–755 and D229–D244.
(21) KANAZAWA, K., MILLER, K. J., and BROWN, M. W. (1979) Cyclic deformation of 1% CrMoV steel under out-of-phase loads, *Fatigue Engng Mater. Structures*, **2**, 217–228.
(22) HILL, R. (1950) *The mathematical theory of plasticity*, Oxford University Press, Oxford, UK.
(23) REED-HILL, R. E. (1979) *Physical metallurgy principles*, Van Nostrand Reinhold, London.
(24) LEE, S. B. (1985) A criterion for fully reversed out-of-phase torsion and bending, *Multiaxial Fatigue, ASTM STP 853*, ASTM, Philadelphia, PA, pp. 553–568.
(25) BROWN, M. W. and MILLER, K. J. (1979) Biaxial cyclic deformation behaviour of steels, *Fatigue Engng Mater. Structures*, **1**, 93–106.